文章编号:0258-7106(2002)03-0240-06

安徽凤阳和张八岭地区含金石英脉的$^{40}Ar/^{39}Ar$年龄及其地质意义*

应汉龙 刘秉光
(中国科学院地质与地球物理研究所,北京 100029)

摘 要 用快中子活化法测定了安徽凤阳和张八岭地区朱顶、毛山和上成3个金矿床第一阶段晚期和第二阶段的含金石英脉,石英的阶段加热$^{40}Ar/^{39}Ar$坪年龄值域为(116.1±0.6~118.3±0.5) Ma,分别与其最小视年龄和等时线年龄接近。坪年龄、最小视年龄和等时线年龄3种年龄值域为(113.4±0.4~118.3±0.5) Ma,可以作为石英的形成年龄域。根据含金石英脉和围岩的空间关系,该年龄值域作为石英脉金矿的形成年龄是合理可靠的。金矿床形成于早白垩世阿普特期,与此时郯庐断裂带略带右行走滑正断层活动一致。

关键词 成矿时代 石英 $^{40}Ar/^{39}Ar$年龄 金矿床 安徽
中图法分类号:P597;P618.51 **文献标识码**:A

安徽凤阳和张八岭地区含金石英脉发育,形成了荣渡、朱顶、大巩山、毛山和上成等金矿床和大量的金矿点。董法先等(1995)测得荣渡和大巩山金矿床蚀变矿物的Rb-Sr等时线年龄分别为(109.0±4.4) Ma和(153.76±11.2) Ma,两者具有较大的差异,但可以看出金矿床形成于中生代晚侏罗世至早白垩世。虽然对石英的$^{40}Ar/^{39}Ar$年龄的意义有不同的认识(邱华宁等,1995),但是只要从样品挑选和用量、照射时间、质谱分析及数据处理等方面严格把关,使Cl和过剩氩的干涉降低,就能得到比较可靠的年龄数据。大量的测定结果也表明石英的$^{40}Ar/^{39}Ar$年龄能够代表石英的形成年龄(桑海清等,1994)。成矿年龄的确定对成矿作用的认识具有重要的意义,鉴于前人仅测定了变质岩中金矿床蚀变矿物的形成年龄,而且年龄数据范围较大(董法先等,1995),而凤阳和张八岭地区含金石英脉的围岩包括太古代和元古代变质岩以及中生代侵入岩,为了确定不同围岩的含金石英脉是否为同一时代形成,金矿成矿作用时间在区域上是否一致,本次研究用石英的$^{40}Ar/^{39}Ar$定年方法,直接测定了凤阳和张八岭变质地体中含金石英脉的年龄。

1 区域和矿床地质概况

凤阳地区在大地构造上位于华北克拉通内。该地区第四纪沉积物分布广泛,出露岩石主要为新太古代五河群片麻岩和角闪岩(董法先等,1995)。张八岭地区主要出露新元古代张八岭群变质海相钠质酸性火山岩,其下可能分布角闪岩和混合岩,大地构造上位于大别—苏鲁造山带内(唐永成等,1998)。张八岭地体在中新生代沿北北东走向郯庐断裂带走滑移动至靠近凤阳地体(万天丰等,1996;王小凤等,2000)(图1)。凤阳地区和张八岭地区除分别发育新太古代侵入岩和新元古代火山岩外,中生代燕山期酸性-基性侵入岩发育,形成女山花岗岩体和管店花岗闪长岩体以及大量的酸性-基性脉岩。这两个地区是郯庐断裂带通过的区域,北北东走向的郯庐断裂带主干断裂及其次级的北北东向、北东向和北西向的断裂发育。含金石英脉主要发育在北北东走向的郯庐断裂带的次级断裂中,少数发育在北西向和北东向的次级断裂中,围岩为五河群和张八岭群变质岩以及管店花闪长岩等(董法先等,1995;邱瑞龙,1998;刘建民等,1998;黄德志等,2000)(图1)。

* 本研究受国家重点基础研究项目(编号:G1999043203)和中国黄金学会项目(编号:97-08)的资助
第一作者简介 应汉龙,男,1964年生,副研究员,主要研究矿床学。
收稿日期 2001-08-16;改回日期 2002-04-07。张绮玲编辑。

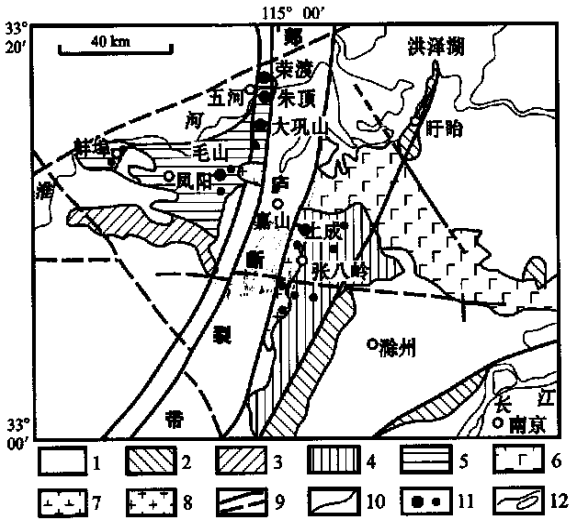

图 1　凤阳-张八岭地区地质及金矿分布简图

1 —新太古界五河群变质岩;2 —新元古界张八岭群变质岩;3 —新元古界-奥陶系沉积岩;4 —震旦系-奥陶系沉积岩;5 —第四系;6 —太古代花岗岩;7 —中生代花岗闪长岩;8 —新生代玄武岩;9 —断裂和推测断裂;10 —地质界线;11 —金矿床和矿点;12 —河流及湖泊

Fig. 1　Geological sketch map showing distribution of gold deposits in Fengyang-Zhangbaling areas

1 —Metamorphic rocks of Neo-Archean Wuhe Group; 2 —Metamorphic rocks of Neoproterozoic Zhangbaling Group; 3 —Neoproterozoic-Ordovician sedimentary rocks; 4 —Sinian-Ordovician sedimentary rocks; 5 —Quaternary; 6 —Archean granite; 7 —Mesozoic granodiorite; 8 —Cenozoic basalt; 9 —Fault and in-ferred fault; 10 —Geological boundary; 11 —Gold deposit and spot; 12 —Rivers and Lakes

根据含金石英脉的空间关系、矿物组合及结构构造,含金石英脉可以划分为 3 个阶段:第一阶段形成贫金的硫化物石英脉;第二阶段形成富金石英硫化物脉;第三阶段形成贫金重晶石碳酸盐石英脉。金矿体主要以脉状和透镜状产于含金石英脉及其两侧的蚀变岩石中,走向与赋矿断裂一致。矿体长度 10 ~ 500 m,延深 10 ~ 450 m,厚度 0.1 ~ 6.5 m,含金 1×10^{-6} ~ 20×10^{-6}。矿石主要为含金富硫化物石英脉,由石英、黄铁矿、黄铜矿、方铅矿、闪锌矿、毒砂、辉铜矿、斑铜矿、辉铋矿、重晶石、自然金、银金矿和碳酸盐矿物组成,围岩蚀变为绢云母化、硅化、绿泥石化、碳酸盐化和粘土化等(董法先等,1995;邱瑞龙等,1998;刘建民等,1998;黄德志等,2000)。

2　样品采集和制备分析

在凤阳地体的毛山、朱顶金矿床和张八岭地区的上成金矿床采集了第一阶段晚期和第二阶段石英集合体样品。毛山金矿床 M2 和朱顶金矿床 Z4 石英采自北北东向的含金石英脉,前者 w_{Au}一般为 1×10^{-6} ~ 15×10^{-6},石英脉的厚度为 0.5 ~ 2 m;后者 w_{Au}一般在 1×10^{-6} ~ 25×10^{-6},石英脉的厚度为 0.3 cm ~ 1.2 m;两者都赋存于五河群变质岩中。上成金矿床的 P2 石英采自北北西向的含金石英脉,w_{Au} 1×10^{-6} ~ 20×10^{-6},脉厚 0.1 ~ 0.4 m,上部赋存于张八岭群变质岩中,下部赋存于管店花岗闪长岩中。石英样品的选择和加工过程参照桑海清等(1994)。

样品在中国原子能科学研究院 49-2 反应堆 H8 孔道中心位置照射,照射时间为 55 h 28 min,瞬间中子通量为 6.63×10^{12} n/(cm^2·s),积分中子通量为 1.32×10^{18} n/cm^2,照射参数 J = 0.01219。样品的前处理、阶段加热和质谱分析在中国科学院地质与地球物理研究所 Ar-Ar 定年实验室进行,测定仪器为 RGA-10 气体源质谱计,其流程以及数据处理见桑海清等(1994)和王松山等(1985);采用的国际标样 BSP-1 角闪石,t = (2 026 ±8) Ma;中国标样 ZBH-25 黑云母,t = (132.7 ±1.2) Ma;ZBJ 角闪石,t = (132.8 ±1.4) Ma。

3　分析结果

3 个金矿床的石英样品在低温阶段(M2:450 ~ 570 ℃;Z4:430 ~ 560 ℃;P2: 430 ~ 660 ℃)和高温阶段(M2:1 100 ~ 1 550 ℃;Z4 和 P2:1 200 ~ 1 550 ℃),^{39}Ar析出率较低,给出的视年龄不具地质年代学意义(表 1);其余 5 个加热阶段的析出率较高,M2、Z4 和 P2 石英样品的^{39}Ar析出量分别达到 77.06 %,80.83 %和 76.62 %(表 1),所获得的$^{40}Ar/^{39}Ar$年龄谱均为宽阔的"马鞍形"(图 2),M2、Z4 和 P2 石英的坪年龄分别是(117.4 ±0.5) Ma、(116.1 ±0.6) Ma 和(118.3 ±0.5) Ma,最小视年龄分别为(116.6 ±0.8) Ma、(114.7 ±0.7) Ma 和(117.1 ±0.8) Ma。对构成坪年龄的 5 个加热阶段的数据进行$^{40}Ar/^{36}Ar$-$^{39}Ar/^{36}Ar$等时线年龄计算,相关系数均在 0.999 以上,年龄分别是(115.0 ±0.2) Ma、(113.4 ±0.4) Ma 和(116.5 ±0.3) Ma。典型的马鞍形年龄谱表明用于定年的石英中确实存在过剩氩。但是,马鞍形年龄谱底部的几组年龄组成的坪年龄接近或略高于矿物的结晶年龄(Zeitler et al., 1986; Lanphere et al.,

表 1 金矿床石英^{40}Ar-^{39}Ar 快中子活化年龄数据

Table 1 $^{40}Ar/^{39}Ar$ fast neutron activation age data of quartz from the gold deposits

地区 加热阶段	温度 t/℃	$(^{40}Ar/^{39}Ar)_m$	$(^{36}Ar/^{39}Ar)_m$	$(^{37}Ar/^{39}Ar)_m$	$(^{38}Ar/^{39}Ar)_m$	$^{39}Ar_K$/ 10^{-12} mol	$(^{40}Ar/^{39}Ar_K)$ ±1 σ	$^{39}Ar_K$/ %	视年龄(t ±1 σ)/ Ma
毛山 M2									
1	450	40.31	0.1085	0.2617	0.3643	0.21	8.409 ±3.25	2.03	176.1 ±38.2
2	570	26.684	0.0673	0.2173	0.3368	0.45	6.888 ±1.42	3.44	145.5 ±13.9
3	680	10.625	0.0161	0.1005	0.1303	1.21	5.624 ±0.23	9.99	119.6 ±1.8
4	760	7.879	0.0081	0.0961	0.1384	2.21	5.492 ±0.12	17.7	116.9 ±1.0
5	840	7.045	0.0053	0.1015	0.1256	3.06	5.475 ±0.01	23.5	116.6 ±0.8
6	920	8.137	0.0088	0.1173	0.1794	2.37	5.538 ±0.13	18.2	117.9 ±1.1
7	1 000	12.558	0.0232	0.2331	0.3093	0.91	5.735 ±0.32	7.67	121.9 ±2.6
8	1 100	16.932	0.0338	0.3085	0.3908	0.75	6.999 ±0.87	5.71	147.7 ±5.7
9	1 200	20.879	0.0439	0.3223	0.4286	0.63	7.986 ±0.87	4.87	167.6 ±9.8
10	1 350	27.594	0.0637	0.3136	0.4623	0.49	8.902 ±1.52	3.78	185.9 ±18.4
11	1 550	38.889	0.0980	0.3811	0.6078	0.35	10.11 ±3.02	2.73	209.6 ±41.9
朱顶 Z4									
1	430	45.688	0.1284	0.1783	0.3303	0.25	7.918 ±4.17	2.16	166.2 ±46.4
2	560	35.401	0.0985	0.1941	0.2847	0.32	6.424 ±2.51	2.72	136.0 ±22.9
3	660	10.459	0.0165	0.091	0.1082	1.26	5.587 ±0.22	10.8	118.8 ±1.8
4	750	7.989	0.0086	0.0917	0.1126	2.02	5.431 ±0.13	17.3	115.8 ±1.0
5	830	7.073	0.0057	0.0848	0.113	2.85	5.386 ±0.1	24.2	114.7 ±0.8
6	900	9.938	0.0082	0.1044	0.1206	2.25	5.501 ±0.13	19.2	117.1 ±1.0
7	1 050	11.956	0.0217	0.1623	0.1978	1.07	5.563 ±0.29	9.13	118.4 ±2.3
8	1 200	18.135	0.0381	0.3017	0.4102	0.68	6.702 ±0.66	5.85	141.5 ±6.3
9	1 350	22.449	0.0481	0.2839	0.4612	0.57	8.078 ±1.01	4.86	169.4 ±11.4
10	1 550	33.427	0.0815	0.4138	0.5786	0.41	9.523 ±2.23	3.53	198.1 ±29.4
上成 P2									
1	450	39.661	0.1102	0.3034	0.3644	0.27	7.271 ±3.15	2.36	153.4 ±32.4
2	560	27.659	0.0718	0.2884	0.3617	0.44	6.562 ±1.53	3.76	138.8 ±14.3
3	660	19.73	0.0450	0.2434	0.2788	0.62	6.048 ±0.78	5.39	128.3 ±6.7
4	760	11.458	0.0198	0.1449	0.1646	1.11	5.633 ±0.26	9.61	119.8 ±2.14
5	840	7.037	0.0052	0.0932	0.117	3.13	5.499 ±0.01	27	117.1 ±0.8
6	920	7.665	0.0070	0.108	0.1364	2.48	5.592 ±0.12	21.4	119.0 ±1.0
7	1 000	10.182	0.0154	0.1897	0.2509	1.27	5.644 ±0.21	11	120.1 ±1.7
8	1 100	13.421	0.0263	0.2611	0.3263	0.88	5.702 ±0.36	7.61	121.2 ±3.0
9	1 200	22.553	0.0532	0.4179	0.5404	0.54	6.962 ±1.02	4.7	147.0 ±17.1
10	1 350	28.03	0.0682	0.5218	0.6616	0.46	8.05 ±1.57	3.96	168.9 ±17.8
11	1 550	34.193	0.8710	0.3102	0.6	0.36	8.625 ±2.34	3.1	180.4 ±28.1

注：λ=5.543e-10/年。下角标 m 表示质谱计测定；K 表示由钾变成的。

1996；Lippolt et al.，1986)。本次研究样品的最小视年龄、坪年龄和等时线年龄非常接近，初始值$(^{40}Ar/^{39}Ar)_i$ 在 304.3 ±4.36 ~ 308.9 ±5.25 之间(图 2)，与尼尔值(295.5)接近。石英脉形成后没有受到后期地质作用影响，可以排除氩丢失的可能性。坪年龄可以代表石英的形成年龄，但从等时线年龄全部小于其相应坪年龄来看，等时线年龄可能更接近于石英的结晶年龄。为慎重起见，取所有年龄数据的域(113.4 ±0.4 ~ 118.3 ±0.5) Ma 作为石英的形成年龄域。

4 地质意义

凤阳和张八岭地区金矿床石英$^{40}Ar/^{39}Ar$ 年龄在误差范围内与荣渡金矿床蚀变矿物的 Rb-Sr 等时线年龄一致，但小于大巩山金矿床蚀变矿物的 Rb-Sr 等时线年龄(董法先等，1995)。其中，上成金矿床含金石英脉石英的$^{40}Ar/^{39}Ar$ 年龄小于管店花岗岩体

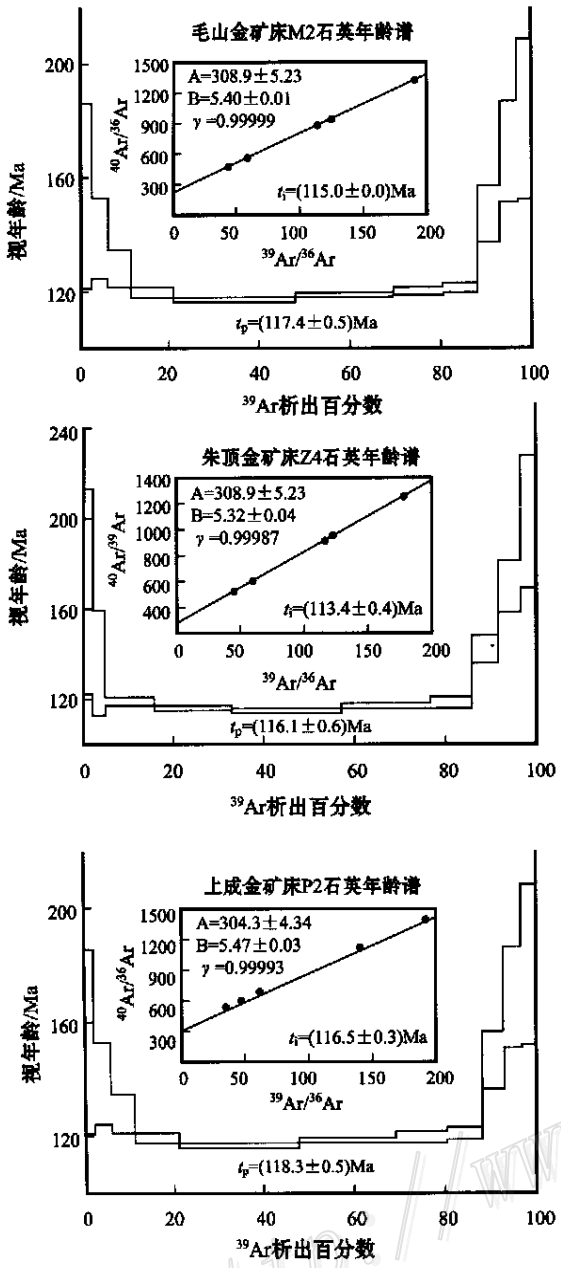

图 2　毛山、朱顶和上成金矿床石英的$^{40}Ar/^{39}Ar$同位素年龄图

Fig. 2　$^{40}Ar/^{39}Ar$ age maps of quartz from the Maoshan, Zhuding and Shangcheng gold deposits

锆石铀-钍-铅法年龄 128 Ma(李学明等,1985),由于含金石英脉深部赋存于管店岩体中,因此石英的$^{40}Ar/^{39}Ar$年龄值是合理的。凤阳和张八岭地区含金石英脉石英的$^{40}Ar/^{39}Ar$年龄作为该地区金矿床的成矿年龄是可靠的。含金石英脉中石英的$^{40}Ar/^{39}Ar$测试结果说明,虽然凤阳和张八岭两个变质地体的地质构造性质不同,但其中金矿成矿年龄基本一致,范围为(113.4±0.4~118.3±0.5) Ma,矿床形成于早白垩世阿普特期,表明这两个地区金矿床成矿作用与同一地质构造作用有关。凤阳和张八岭地体金矿床的成矿作用时间略晚于郯庐断裂带中段东侧的胶东地体中金矿的成矿时代 126.1 Ma(杨进辉等,2000)。

郯庐断裂带在白垩纪以前主要为左行走滑活动,为压扭性质,早白垩世为呈略带右行走滑的正断层活动,这一阶段为拉张性质,岩浆活动强烈。研究表明形成金矿床的成矿流体中岩浆热液成分十分重要(董法先等,1995;邱瑞龙,1998),说明凤阳和张八岭地区金矿成矿作用与郯庐断裂带拉张作用和岩浆作用有一定关系,金矿床是在拉张的动力背景下形成的。郯庐断裂带的拉张活动活动为岩浆作用和金矿成矿作用提供了动力和空间。

致　谢　野外工作得到安徽省黄金管理局、凤阳县黄金公司和五河县黄金公司的帮助。安徽省地质资料处提供了研究区部分研究报告。桑海清和裘冀完成了样品测试。审稿人和编辑对原稿提出许多修改建议。在此一并诚表谢意。

References

Dong F X, Li Z J, Chen B L, et al. 1995. The structural control of gold deposits and their exploration in the Dagongshan-Rongdu area of Wuhe county, Anhui Province [M]. Beijing: Geological Publishing House. 1~171 (in Chinese with English abstract).

Huang D Z, Dai T G, Kong H, et al. 2000. Study on origin of ore-forming fluid of quartz-vein-type deposits in Zhangbaling tectonic zone, Anhui [J]. Geotectonica and Metallogenia, 24: 231~236 (in Chinese with English abstract).

Lanphere M and Dalrymple G B. 1976. Identification of excess ^{40}Ar by the $^{40}Ar/^{39}Ar$ age spectrum technique [J]. Earth Planet. Sci. Lett., 32: 141~148.

Li X M, Li B X, Zhang Y, et al. 1985. Isotopic age of Guandian intrusion and dynamic metamorphism of Tanlu fault zone[J]. Journal of University of Science & Technology of China, (Supp.): 254~259 (in Chinese with English abstract).

Lippolt H J, Fuhrmann U and Hradetzky H. 1986. $^{40}Ar/^{39}Ar$ age determination of sanidines of the Eifei volcanic field (Federal Republic of Germany): constraints on age duration of a Middle Pleistocence cold period [J]. Chem. Geol. (Isot. Geosci. Sect.), 59: 187~204.

Liu J M, Chen B L, Meng X G, et al. 1998. Geological and geochemical properties of Dagongshan gold deposit, Wuhe, Anhui, and its

genesis [J]. Mineral Deposits, 17(Supp.): 303 ~ 306 (in Chinese).

Qiu H N, Dai T M and Pu Z P. 1995. The implication of spectra of trace K minerals from the Lushui tengsten-tin deposit, Yunnan Province[J]. Mineral Deposits, 14(3): 273 ~ 280 (in Chinese with English abstract).

Qiu R L. 1998. Geology and geochemistry of gold deposits in Zhangbaling region [J]. Mineral Deposits, 17(Supp.): 335 ~ 338 (in Chinese).

Sang H Q, Wang S S, Hu S L, et al. 1994. $^{40}Ar/^{39}Ar$ dating method and Ar isotope mass spectrometry analysis of quartz [J]. Journal of Chinese Mass Spectrometry Society, 15(2): 17 ~ 27 (in Chinese with English abstract).

Tang Y C, Wu Y C, Chu G Z, et al. 1998. Geology of copper-gold polymetallic deposits in the along-Changjiang area of Anhui Province [M]. Beijing: Geological Publishing House. 1 ~ 351 (in Chinese with English abstract).

Wan T F, Zhu H, Zhao L, et al. 1996. Formation and evolution of Tancheng-Lujiang fault zone: A review[J]. Geosciences, 10(2): 159 ~ 167 (in Chinese with English abstract).

Wang S S, Sang H Q, Hu S L, et al. 1985. Application of the 49-2 reactor to $^{40}Ar/^{39}Ar$ dating and the geological significance of age spectra of amphibolite from Caozhuang Group, Qian'an[J]. Acta Petrologica Sinica, 2(2): 36 ~ 42 (in Chinese with English abstract).

Wang X F, Li Z J, Chen B L, et al. 2000. Tan-Lu fault belt [M]. Beijing: Geological Publishing House, 1 ~ 374 (in Chinese with English abstract).

Yang J H and Zhou X H. 2000. The Rb-Sr isochron of ore and pyrite sub-samples from Linglong gold deposit, Jiaodong Peninsula, eastern China, and their geological significance[J]. Chinese Science Bulletin, 45(24): 2272 ~ 2277.

Zeitler P K and Gerald J D F. 1986. Saddle-shaped $^{40}Ar/^{39}Ar$ age spectra from young, microstructurally complex potassium feldspars [J]. Geochim. Cosmochim. Acta, 50: 1185 ~ 2119.

附中文参考文献

董法先, 李中坚, 陈柏林, 等. 1995. 安徽五河县大巩山-荣渡地区金矿控矿构造和找矿方向[M]. 北京: 地质出版社. 1 ~ 176.

黄德志, 戴塔根, 孔 华, 等. 2000. 安徽张八岭构造带石英脉型金矿成矿流体来源研究[J]. 大地构造与成矿学, 24(3): 231 ~ 236.

李学明, 李彬贤, 张 翼, 等. 1985. 安徽管店岩体的同位素地质年龄和郯庐断裂带的动力变质作用[J]. 中国科技大学学报, (增刊): 254 ~ 261.

刘建民, 陈柏林, 孟宪刚, 等. 1998. 安徽五河大巩山金矿床地质地球化学特征及矿床成因[J]. 矿床地质, 17(增刊):303 ~ 306.

邱华宁, 戴潼谟, 蒲志平. 1995. 云南泸水钨锡矿床微量钾矿物 ^{40}Ar-^{39}Ar 马鞍形年龄谱的含义[J]. 矿床地质, 14(3): 273 ~ 280.

邱瑞龙. 1998. 张八岭地区金矿地质及矿床地球化学[J]. 矿床地质, 17(增刊): 335 ~ 338.

桑海清, 王松山, 胡世玲, 等. 1994. 石英的 $^{40}Ar/^{39}Ar$ 定年方法及 Ar 同位素质谱分析[J]. 质谱学报, 15(2): 17 ~ 27.

唐永成, 吴言昌, 储国正, 等. 1998. 安徽沿江地区铜金多金属矿床地质[M]. 北京: 地质出版社. 1 ~ 351.

万天丰, 朱 鸿, 赵 磊, 等. 1996. 郯庐断裂带的形成和演化:综述[J]. 现代地质, 10(2):159 ~ 167.

王松山, 桑海清, 胡世玲, 等. 1985. 应用 49-2 反应堆进行 $^{40}Ar/^{39}Ar$ 定年及迁安曹庄群斜长角闪岩年龄谱的地质意义[J]. 岩石学报, 2(3):36 ~ 42.

王小凤, 李中坚, 陈柏林, 等. 2000. 郯庐断裂带[M]. 北京: 地质出版社. 1 ~ 374.

杨进辉, 周新华. 2000. 胶东地区玲珑金矿矿石和载金矿物 Rb-Sr 等时线年龄与成矿时代[J]. 科学通报, 5(14):1547 ~ 1552.

$^{40}Ar/^{39}Ar$ Dating of Gold-bearing Quartz Veins in Fengyang and Zhangbaling Areas, Anhui Province, and Its Geological Significance

Ying Hanlong and Liu Bingguang

(Institute of Geology and Geophysics, Chinese Academy of Sciences, Beijing 100029, China)

Abstract

Tectonically Fengyang and Zhangbaling areas belong respectively to the North China craton and the Dabie orogene, with Neo-Archean gneiss and amphibolite and metamorphosed marine facies sodic volcanic rocks being the main outcrops respectively. The Zhangbaling terrane strike-skipped along the Tan-Lu fault zone in Mesozoic and Cenozoic and got close to the Fengyang terrane. Mesozoic Yanshanian intrusions occur extensively in the two areas. Gold-bearing quartz veins occur in metamorphic rocks in Fengyang area and in granodiorite and metamor-

phosed marine facies sodic volcanic rocks in Zhangbaling area. Generally, three stages of quartz veins can be recognized, i.e., gold-deficient sulfide quartz veins, gold-rich quartz sulfide veins and gold-deficient barite and/or carbonate veins. The $^{40}Ar/^{39}Ar$ step-heating plateau ages of the late first-stage and the second-stage quartz aggregates from the Zhuding, Maoshan and Shangcheng gold deposits range between 116.1 ~ 0.6 Ma and 118.3 ~ 0.5 Ma and are quite close to their least apparent ages and isochronal ages respectively. All plateau, least apparent and isochronal ages range from 113.4 ~ 0.4 Ma to 118.3 ~ 0.5 Ma, considered to be the formation age range of the quartz. It is reasonable and reliable to take the $^{40}Ar/^{39}Ar$ age range of the quartz as the formation age range of gold-bearing quartz veins on the basis of spatial relationship between gold-bearing quartz veins and their country rocks. The gold deposits in the two areas were formed in Aptian Stage of Cretaceous, when the Ta-Lu fault zone moved as a normal fault with slightly right-lateral strike-skip, extended and had very strong magmatic activity. It is shown that the magmatic hydrothermal fluid is a very important component part in the ore-forming hydrothermal fluid in Fengyang and Zhangbaling areas. The gold ore deposits in Fengyang and Zhangbaling areas genetically related to the extensional movement of the Ta-Lu fault zone and the magmatic activity were formed under the extensional dynamic condition in Late Cretaceous. Therefore, the extensional movement of the Ta-Lu fault zone provided energy and space for magmatic and gold ore-forming processes.

Key words: formation age, quartz, $^{40}Ar/^{39}Ar$, gold deposit, Anhui

---

(上接第 263 页)(Continued from p.263)

and granite (0.21 and 0.26 respectively) indicate the efficiency of transfer of thermal energy to mechanical (explosive) energy from the interaction of hot magma with cold water is higher than 90 %. This serves as geochemical evidence for magma-exotic water mixing model of cryptoexplosive breccia. The $\delta^{34}S$ of ore-stage sulfide and $\delta^{31}C$ of ore-stage calcite show that the S and C are derived from the deep source, whereas the post-ore $\delta^{34}S$ and $\delta^{31}C$ are possessed of mixing source. These Pb isotopes of country rock (volcanic rock) and basement rock (granite and metamorphic rock) belong to anomalous Pb enriched in radioactive lead and constitute a linear array with Pb isotopes of K-feldspar, pyrite and galena. This implies that the ore-forming material (uranium) is characterized by multisource from host rock and basement rock.

Key words: stable isotope, water/rock ratio, magma-exotic water mixing explosive model, cryptoexplosive breccia, uranium deposit

---

(上接第 277 页)(Continued from p.277)

gangue minerals (quarts, celestine, calcite and gypsum) shows that the homogenization temperatures range from 52 ℃ to 309 ℃, clustered around 110 ~ 150 ℃, with salinities of 5.09 % ~ 19.63 % wt NaCl equivalent. The pressure was 32.5 ~ 22.6 MPa, corresponding to an ore-forming depth of 0.9 ~ 1.5 km.

Key words: stratigraphical and structural control, Pb and S isotope, homogenization temperature, salinity, Jinding Pb-Zn deposit